Weakly Ionized Nonequilibrium Viscous Shock-Layer and Electrostatic Probe Characteristics

PAUL M. CHUNG*
Aerospace Corporation, San Bernardino, Calif.

The electrochemical interactions between the hypersonic stream of weakly ionized gases and the stagnation region of electrically biased blunt bodies are analyzed. The analysis is based on a continuum description. From the study, typical current-potential relationships for electrostatic stagnation probes are obtained. The effects on the electrical characteristics of the finite-rate collisional energy exchange between electrons and neutrals, and the nonequilibrium electron-ion recombination are studied. Particular attention is given to the electron temperature variations in the freestream, shock, and the shock layer. Among other things, it was found that the classical electron saturation current is not usually attained.

Nomenclature

A, $\hat{A}$ = defined in Eqs. (30)
B_0, B_1, B_2 = defined in Eqs. (47) and (50)
C = mass fraction
c_p = specific heat at constant pressure
D = binary diffusion coefficient
E, $\hat{E}$ = dimensionless electric field intensities defined in Eqs. (30)
E^* = electric field intensity in y direction
E_v = vibrational energy
e = charge of an electron, except electron in Eqs. (9)
f = dimensionless stream function defined in Eq. (26)
H = $h/h_s = T_g/T_{gs}$
h = total enthalpy of gas mixture
J = dimensionless current density defined by Eq. (51)
j = particle current density toward surface
K = mobility
k = Boltzmann constant
k_R = specific ion-electron recombination coefficient
k_{RO} = constant portion of k_R
L = nose cadius
Le_i = ion Lewis number Pr/Sc_i
l = $(\rho\mu)/(\rho\mu)_s$
M = particle mass
m = C/C_s
n = number density
Pr = Prandtl number of gas mixture
p = total pressure
p_i, p_e = partial pressures of ions and electrons, respectively
Q = electron energy source due to collisions
q = diffusion flux toward surface
Re_s = shock Reynolds number, $-v_sL/\nu_s = \rho_\infty u_\infty L/\mu_s$
T = absolute temperature
Sc_i = ion Schmidt number, $\mu/\rho D_i$
t = time
u = x component of over-all gas velocity (see Fig. 1)
u_∞ = freestream gas velocity toward the body
V = electric potential
v = y component of over-all gas velocity (see Fig. 1)
V_e = total macroscopic velocity of electrons ($= v + v_e$) in y direction
v_e = diffusion velocity of electrons in y direction
$\hat{v}_e$ = moleculer speed of electrons
W = mass source
x = direction and distance along the surface
y = direction and distance normal to the surface
α_2 = mass fraction of molecules
β = $(T_g/T_e)_s$
Γ_1 = Damkohler number for temperature equilibration defined by Eq. (38)
Γ_2 = Damkohler number for ion-electron recombination defined by Eq. (39)
ϵ = ρ_∞/ρ_s
ϵ_0 = permittivity
η = similarity variable defined in Eq. (25)
θ = T_e/T_{es}
θ_v = characteristic vibrational temperature
Λ = Debye shielding length
λ_e = electron thermal conductivity
$\hat{\lambda}$ = mean free path
μ = dynamic viscosity
ν = kinematic viscosity
$\hat{\nu}_{eg}$ = electron-neutral gas collision frequency
ρ = density of gas mixture
σ = collision cross section
$(\ )'$ = differentiation with respect to η

Subscripts†

e = electrons
g = neutral gas
i = ions
0 = before the shock (see Fig. 1)
s = after the shock (see Fig. 1)
w = wall (see Fig. 1)
∞ = freestream
Δ = sheath edge

Received July 14, 1964; revision received December 4, 1964. The author is grateful to M. Grewal and D. Dix of the Aerospace Corporation for their stimulating discussions during the course of preparation of this report.

* Head, Re-entry Fluid Dynamics Department, Office of Research.

I. Introduction

ELECTROSTATIC (Langmuir) probes recently are being employed to study the properties of weakly ionized gases in laboratories. Because of their relative simplicity in construction and usage, a rather large amount of the probe measurements, pertaining to the electron number density and electron temperature, have been obtained.

For many years, numerous theories have been developed to interpret the probe characteristics for various plasma conditions (for instance, see Ref. 1 and the discussion and references given in Ref. 2). Most of the conventional theories, however, are not applicable to the continuum viscous flow regime of weakly ionized gases wherein many of the present-day probes operate. Rather recently, however, a number of analyses have appeared in the literature which studied various important aspects of the electrical characteristics of continuum, weakly ionized gases.

Among the recent studies,‡ the present analysis of stagnation viscous shock layer is more closely related to the bound-

† Symbols in the text without subscripts refer to the over-all gas mixture unless specified otherwise.

‡ Because of space limitation, only those references that are directly related to the present analysis are cited herein. For more complete references, see Ref. 24.

ary-layer problems studied by Talbot,[2] Turcotte,[3] Wilson and Turcotte,[4] Lam,[5] Su,[6] Chung and Mullen,[7] and Chung.[8] In these previous analyses, the following major assumptions, one or more of which are usually not justified in practice, have been made: 1) the electron and ion temperatures are the same, or the ratio of the two temperatures is constant throughout the flow field; 2) electron temperature is known at the boundary-layer edge; 3) chemical reaction of ion-electron recombination is frozen; 4) appreciable charge separation occurs only near the surface where the convection is negligible.

As we shall see subsequently, the electron temperature is seldom in equilibrium with the ion and neutral gas temperatures for gases such as air, and the ratio of the two temperatures is never a constant. The nonequilibrium electron temperature was considered in Ref. 7, but only very approximately. Furthermore, the electron temperature is, for most cases, not known a priori at the boundary-layer edge, particularly when the oncoming plasma stream is supersonic. In fact, because of the high thermal conductivity of electron gas, the electron thermal layer is in a sort of "merged layer" regime§ in that the electron temperature variation in the viscous boundary layer is usually merged with the variations that occur across the shock layer, shock, and in the plasma upstream of the shock. These electron temperature variations are, of course, functions of the electrical potential of the surface and of many other factors. In practice, therefore, assumptions 1 and 2 are not justified. Also, because of the shock and the nonuniform electron temperature field, as well as the electric field that extends much beyond the boundary-layer edge, the boundary-layer analysis alone is usually not sufficient to study the over-all electrical interactions of the ionized gases with a solid surface, as was pointed out in Ref. 8. There are plasma flow regimes wherein assumptions 3 and 4 are justified.[8] However, by eliminating these two assumptions, the regime of applicability of the present analysis can be enhanced substantially.

In many laboratory applications, the flow conditions and the size of the probe are such that the neutral gas flow itself is no longer in a boundary-layer regime but rather in a more rarefied viscous-layer regime. The various stagnation flow regimes of neutral gases have been studied quite thoroughly, for instance, by Hayes and Probstein,[9] Chung,[10] and Cheng.[11]

In the present paper, an analysis will be made on the electrical interactions between a hypersonic stream of weakly ionized gases and an axisymmetric stagnation surface that is electrically biased. The four major assumptions made in the previous papers will be eliminated in the present analysis. Typical potential-current relationships will be established. In order to take into account the major features of the electron temperature variations mentioned earlier, and also in consideration of the many laboratory conditions wherein the neutral gas is somewhat rarefied, the present study will be based on the viscous hypersonic shock-layer model previously employed by Chung[10] and Cheng[11] and also on the electron momentum and energy equations to be developed for the plasma upstream of the shock.

II. Formulation

Let us consider the viscous flows of weakly ionized gases such as air around a spherical nose with the following properties.

1) The degree of ionization and the collision cross sections between the various particles of the gas are such that the collisions between the ionized particles and the neutral particles predominate over those between the ionized gas particles. (This means that the degree of ionization must be smaller than about 10^{-3} for gases such as air.)

2) The distance through which the electrical effects are pronounced, such as the sheath thickness, is much greater than the mean free path for the ionized-neutral gas collisions but is smaller than the (neutral gas) shock-layer thickness.

3) The flow is such that there are many collisions, both ionized-neutral and electron-electron collisions, during the transport of the ionized species across the shock layer.

We shall define such a plasma as a continuum plasma and shall base the analysis of the plasma flow on a complete continuum description. The rigorous justifications of such description which must come from the kinetic theory are not yet available.¶ However, an analysis based on a self-consistent continuum description of the entire plasma flow field is a far more acceptable one than any other existing classical analysis as can be seen from the arguments given in Refs. 5, 6, and 8. The analysis herein is presented, therefore, as that describing the major electrical effects for engineering purposes rather than as an exact theory.

We shall first formulate the governing equations for the viscous shock layer (between the wall and behind the shock). Then we shall formulate those for the shock and the flow upstream of the shock.

Viscous Stagnation Shock Layer

Governing equations

Because the degree of ionization of the gases of the present interest is very small, the over-all continuity, momentum, and energy equations of the plasma are essentially those of the neutral gas and are unaffected by the presence of the ionized species. The hypersonic, viscous, thin shock layers of neutral gases have been analyzed quite thoroughly[9–11] for the stagnation region of axisymmetric blunt bodies. The over-all governing equations are therefore identical to those given in Ref. 10, except that the netural gas reaction is assumed to be frozen, and are not reproduced here. The assumption of frozen neutral gas reaction is justified for the laboratory applications because the neutral gas-phase reaction, which is predominantly of atom recombination since the oncoming stream is predissociated, is usually frozen for small probe sizes of the present interest.[13]

For the ionized species, we formulate the conservation equation for the ions,** the conservation and energy equations for the electrons, and the Poisson equation as follows. These equations are essentially those derived in Ref. 7 except the ion and electron source terms are added, and, as we shall see subsequently, the electron diffusion flux term is modified to take more accurate account of the transport processes:

Ion Conservation

$$\rho v(dC_i/dy) = (d/dy)(q_i - \rho K_i E^* C_i) + W_i \tag{1}$$

Electron Conservation

$$\rho v(dC_e/dy) = (d/dy)(q_e + \rho K_e E^* C_e) + W_e \tag{2}$$

Poisson

$$dE^*/dy = \rho(e/\epsilon_0)[(C_i/M_i) - (C_e/M_e)] \tag{3}$$

Electron Energy

$$[\rho v C_e - (q_e + \rho K_e E^* C_e)]\left(c_{pe}\frac{dT_e}{dy} + \frac{1}{M_e}eE^*\right) = \frac{d}{dy}\left(\lambda_e\frac{dT_e}{dy}\right) + Q \tag{4}$$

§ Even when the neutral gas flow is in boundary-layer regime.

¶ Some attempts are being made recently (see, for instance, Ref. 12).

** All the positive ions are grouped together.

The electron energy equation can also be cast into various other forms (see, for instance, Refs. 14 and 15). The ion temperature is assumed to be equal to the neutral gas temperature.

We shall now describe and derive the diffusion flux terms q_i and q_e, the mass and the energy source terms W_i, W_e, and Q, and the transport coefficients. Other terms of the equations have been discussed in Refs. 7 and 8.

Diffusion fluxes

A generalized diffusion process can be thought of as that occurring due to a gradient of hydrostatic imbalance. The diffusion fluxes of ions and electrons can thus be expressed as[15]

$$q_i = \frac{M_i D_i p}{kT_g} \frac{d[(p_i/p)]}{dy} \tag{5}$$

$$q_e = \frac{M_e D_e p}{kT_e} \frac{d[(p_e/p)]}{dy} \tag{6}$$

Equations (5) and (6) become, for the weakly ionized gases wherein $(n_e/n_g)(T_e/T_g) \ll 1$,

$$q_i = \rho D_i (dC_i/dy) \tag{7}$$

$$q_e = \rho D_e \frac{1}{(T_e/T_g)} \frac{d[C_e(T_e/T_g)]}{dy} \tag{8}$$

Ion and electron source terms

Let us consider that the freestream is comprised of air that is preionized to a substantial degree such that a further ionization in the highly cooled shock layer is negligible in comparison with the electron-ion recombination. Up to the static enthalpy of about 300RT, the major ionized species of air are NO^+, O_2^+, N_2^+, and electrons. It was shown by Lin and Teare[16] that the specific recombination coefficients for the reactions involving these ionized species

$$\begin{aligned} NO^+ + e &\rightarrow N + O \\ O_2^+ + e &\rightarrow O + O \\ N_2^+ + e &\rightarrow N + N \end{aligned} \tag{9}$$

are all about the same and may be expressed as

$$k_R = 3 \times 10^{-3}\, T_e^{-3/2}\ \text{cm}^3/\text{sec} \tag{10}$$

The three recombination processes given in Eqs. (9) can therefore be grouped together, and we may write, for the over-all W_i and W_e,

$$(W_i/\rho)M_e = (W_e/\rho)M_i = -k_R \rho C_i C_e \tag{11}$$

Electron energy source term

First, it is seen that the particular electron-ion recombination processes given by Eqs. (9) create neither energy sources nor sinks for unit mass of electrons. The electron energy source term Q is, hence, comprised of the energy exchanges between the electrons and the neutral gas particles by elastic collisions and by those inelastic collisions that change the internal energy levels of the neutral gas particles. It is clear from the boundary-layer analysis of Ref. 7 that the energy exchange by the elastic collisions can be neglected for most of the laboratory applications. We shall therefore briefly consider the remaining energy exchange mechanism, which is the inelastic collisions.

The maximum energy of electrons concerned in the present analysis is about 1 or 2 ev. It can be seen that (for instances, see Refs. 17 and 18) the most probable inelastic energy exchanges for these electron energy levels are those that occur between the electrons and the various vibrational states of the oxygen and nitrogen molecules. We shall herein formulate a suitable expression for Q based on the energy exchange between the electrons and the vibrational states of the molecular species.

The energy exchange rates between the translational energy of the electrons and the vibrational energies of the molecules can be expressed as [19]

$$dE_v/dt = (1/\tau_v)[E_v(T_e) - E_v(T_v)] \tag{12}$$

where the vibrational relaxation time τ_v is given by

$$1/\tau_v = \hat{\nu}_{eg} p^{1\rightarrow 0}(1 - e^{-\theta_v/T_v}) \tag{13}$$

$p^{1\rightarrow 0}$ is the probability per collision for de-excitation from the first to the ground vibrational state of the molecules. Some estimates of $p^{1\rightarrow 0}$ for O_2 and N_2 can be obtained from the literatures such as Refs. 17 and 18. Now we assume that the vibrational temperature of the molecules is in equilibrium with the translational temperature of the neutral gas and the ions. Then for the shock layers wherein T_g is mostly greater than θ_v, Eqs. (12) and (13) can be combined to give

$$Q/\rho = -\tfrac{1}{2}\alpha_2 k(\sigma_{eg}\hat{v}_e/M_e M_g) p^{1\rightarrow 0}(1 - e^{-\theta_v/T_g}) \rho C_e (T_e - T_g) \tag{14}$$

Diffusion coefficients and electron thermal conductivity

General expressions for the transport coefficients are given by Fay.[20] The following relationships are derived herein for the weakly ionized air by noting from Hansen[21] that the collision cross sections between the ionized species and the neutral gas particles vary approximately with $1/T^{1/2}$ and $\sigma_{eg}/\sigma_{gg} \approx \frac{1}{2}(T_g/T_e)^{1/2}$

$$D_e/D_i = (T_e/T_g)(M_i/M_e)^{1/2} \tag{15}$$

$$\lambda_e = \frac{5k}{M_e} \frac{1}{Pr} \left(\frac{M_i}{M_e}\right)^{1/2} \mu \left(\frac{T_e}{T_g}\right) C_e \tag{16}$$

Now, all the terms of the governing equations for the shock layer which have not been described in the previous works[7, 8, 10] have been discussed. The boundary conditions will be discussed later in the "Analysis of Equations."

Shock and Flow Upstream of Shock

Let us consider a uniform supersonic stream of weakly ionized gas passing through a normal shock. First, let us consider that no applied electric field is present. Although the over-all flow upstream of the shock may be considered as supersonic, the electron gas flow is for most cases subsonic†† and, strictly speaking, only the neutral gas and ions are shocked and compressed directly. The compression of ions without the compression of electrons, however, creates a strong electric field in accordance with the Poisson equation, Eq. (3). This electric field immediately compresses the electrons to the number density corresponding to that of ions, thus preserving the over-all neutrality of the plasma. An analysis, therefore, of the electron energy relation across the shock is necessary to determine the electron temperature behind the shock unless the electron temperature is always in equilibrium with the neutral gas temperature. The electron temperature profiles for normal shocks without any solid body and applied electric field have been studied by several investigators. One of the most recent studies on the subject is that carried out by Grewal and Talbot.[22]

We shall now formulate the governing equations for the electrons between just behind the shock (point s in Fig. 1) and the freestream, assuming that the probe is a sphere. The collisional energy exchange between the electrons and the neutral gas particles, and the chemical reactions involving the ionized species, are negligible in the upstream of the shock

†† Actually, the present analysis is limited to the cases in which the electron flow is subsonic.

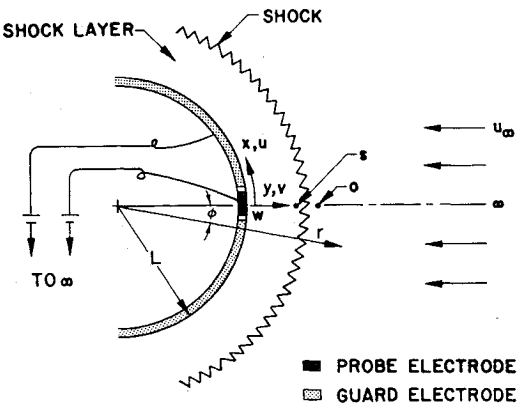

Fig. 1 Flow configuration.

as compared with those in the viscous shock layer. Therefore, these processes are considered to be frozen. In a general form we have the following equations:

Continuity

$$\nabla \cdot (n_e \mathbf{V}_e) = \nabla \cdot (n_e \mathbf{v}_e) = 0 \tag{17}$$

Momentum

$$\nabla p_e + e n_e \mathbf{E}^* = -\mathbf{v}_e n_e (kT_e/D_e) \tag{18}$$

Energy

$$n_e \mathbf{V}_e \cdot [\tfrac{5}{2} k \nabla T_e + e\mathbf{E}^*] = \nabla \cdot (\lambda_e \nabla T_e) \tag{19}$$

In deriving the electron momentum equation, we made use of the fact that the convection terms are negligible after Grewal and Talbot.[22] Noticing from Eq. (15) that $T_e/D_e = (T_e/D_i)(M_e/M_i)^{1/2}$ is constant in the inviscid region, and also with the aid of Eq. (17), we take the divergence of Eq. (18) and obtain

$$\nabla^2 \Psi = 0 \tag{20}$$

where the scalar function Ψ is defined by

$$\nabla \Psi = \nabla p_e + e n_e \mathbf{E}^* \tag{21}$$

Combining Eqs. (18) and (19) we derive,

$$k n_e \mathbf{V}_e \cdot [\tfrac{3}{2} \nabla T_e - T_e (\nabla n_e / n_e) - (T_e/D_e)\mathbf{v}_e] = \nabla \cdot (\lambda_e \nabla T_e) \tag{22}$$

Now Eqs. (20) and (22) become as follows for the vicinity of the stagnation line in a spherical coordinate (see Fig. 1):

Momentum

$$\frac{\partial^2 \Psi}{\partial r^2} + \frac{2}{r}\frac{\partial \Psi}{\partial r} + \frac{1}{r^2}\frac{\partial^2 \Psi}{\partial \phi^2} + \frac{1}{r^2}(\cot\phi)\frac{\partial \Psi}{\partial \phi} = 0 \tag{23}$$

Energy

$$k n_e V_e \left[\frac{3}{2}\left(\frac{\partial T_e}{\partial r}\right) - \frac{T_e}{n_e}\left(\frac{\partial n_e}{\partial r}\right) - v_e\left(\frac{T_e}{D_e}\right)\right] = \frac{\partial}{\partial r}\left(\lambda_e \frac{\partial T_e}{\partial r}\right) + \lambda_e \frac{2}{r}\frac{\partial T_e}{\partial r} + \frac{1}{r^2}\frac{\partial}{\partial \phi}\left(\lambda_e \frac{\partial T_e}{\partial \phi}\right) + \frac{\lambda_e}{r^2}(\cot\phi)\frac{\partial T_e}{\partial \phi} \tag{24}$$

The preceding two equations are elliptic such that a complete description of the boundary conditions all around the body, as well as everywhere in the freestream, is needed to obtain the exact solution. This obviously is a near impossible task and, moreover, such an exact solution is not warranted for the present purpose. A large electric field penetrates beyond a viscous region, and hence the equations such as Eqs. (23) and (24) become important primarily when the surface is drawing a large amount of electron current as was pointed out in Ref. 8. Under such circumstances, the electron temperature in the inviscid region is largely governed by the surface potential rather than the shock. With this in mind, we consider that the entire probe surface (both probe and guard electrode surfaces) is equipotential. Then the variations of electron temperature in the ϕ direction (see Fig. 1) will be much smaller than those along the stagnation line, and the last two terms of Eqs. (23) and (24) may be neglected for the present analysis along the stagnation line. It is pointed out here that, according to Eq. (23) and the work of Ref. 5, the thickness of the region directly influenced by the applied electric field is of order L. In this region, for instance, the effect of a nonuniform electric field along the surfaces of $\phi > \pi/2$ on the field intensities near the forward stagnation line is to change them by about 10%. With their last two terms neglected, Eqs. (23) and (24) are now ordinary differential equations and are amenable to approximate analyses.

III. Analysis of Equations

The electron temperature behind the shock is not known a priori. Hence, when a freestream condition is specified, the direct analysis requires a simultaneous solution of the governing equations of the shock layer and the electron energy equation between s and ∞. Instead of solving the direct problem, for convenience, we shall solve a sort of "inverse" problem in the following manner.

First, the governing equations for the shock layer will be transformed into the form similar to that employed in Ref. 10. The resulting equations will be solved for various shock boundary conditions, including arbitrarily assigned T_{es}, by the use of a digital computer for they are not amenable to a complete analytical treatment. The approximate electron energy equation between just behind the shock and the freestream will then be integrated analytically. The freestream conditions corresponding to each of the shock-layer solutions will then be determined. Among other conveniences, this inverse procedure has an advantage in that the same numerical solutions of the shock-layer equations can still be used should the upstream geometry, with respect to the electric field, change or should one decide to make a more exact account of the region upstream of the shock as compared to the present analysis. Finally, from the results, typical current-potential relationships will be established between the surface and the freestream.

Viscous Shock Layer

We first define the following nondimensional variables after Chung[10] where $(\,)'$ denotes the differentiation with respect to η:

$$\eta = \frac{2^{1/4}}{L}(\epsilon Re_s)^{1/2}\int_0^y \frac{\rho}{\rho_\infty}\,dy \tag{25}$$

$$f = -2^{-5/4}(\epsilon Re_s)^{1/2}(\rho v/\rho_\infty u_\infty) \tag{26}$$

$$f' = (1/2^{1/2})(L/u_\infty)(\partial u/\partial x) \tag{27}$$

$$H = h/h_s \tag{28}$$

Also, we define the following additional nondimensional variables and parameters:

$$m_i = C_i/C_{is} \qquad m_e = C_e/C_{es} \qquad \theta = T_e/T_{es} \tag{29}$$

$$\left.\begin{aligned} E &= \frac{\epsilon_0 E^*}{e n_{es} L} \qquad \hat{E} = 2^{1/4}\left(\frac{Re_s}{\epsilon}\right)^{1/2} E \\ A_i &= \frac{e^2 n_{is} L^2}{\epsilon_0 k T_{gs}} = \left(\frac{L}{\Lambda_{is}}\right)^2 \qquad A_e = \frac{e^2 n_{es} L^2}{\epsilon_0 k T_{es}} = \left(\frac{L}{\Lambda_{es}}\right)^2 \\ \hat{A} &= \frac{A}{2^{1/2} Re_s/\epsilon} \end{aligned}\right\} \tag{30}$$

With the particular definition of the nondimensional stream

function f given by Eqs. (26) and (27), the over-all continuity equation[10] is automatically satisfied. The over-all momentum and energy equations[10] and Eqs. (1–4) are transformed with the aid of Eqs. (7, 8, 11, and 14–16) as follows:

Over-All Momentum

$$lf''' + 2ff'' + [H\epsilon(1 - \epsilon) + (f')^2] = 0 \tag{31}$$

Over-All Energy

$$(l/Pr)H'' + 2fH' = 0 \tag{32}$$

Ion Conservation

$$(m_i' - \hat{A}_i\hat{E}m_i)' + 2(Sc_i/l)fm_i' = \Gamma_2\beta^{1.5}(1/\theta^{1.5})(1/H)m_im_e \tag{33}$$

Electron Conservation

$$\left[\left(\frac{\theta}{H}m_e\right)' + \hat{A}_e\hat{E}m_e\right]' + 2\beta\left(\frac{M_e}{M_i}\right)^{1/2}\left(\frac{Sc_i}{l}\right)fm_e' = \Gamma_2\beta^{2.5}\left(\frac{M_e}{M_i}\right)^{1/2}\frac{1}{\theta^{1.5}}\frac{1}{H}m_im_e \tag{34}$$

Poisson

$$\hat{E}' = m_i - m_e \tag{35}$$

Electron Energy

$$\frac{2}{Le_i}\left[\left(\frac{\theta}{H}m_e\right)\theta'' + \left(\frac{\theta}{H}m_e\right)'\theta'\right] + \left[2\beta\left(\frac{M_e}{M_i}\right)^{1/2}\left(\frac{Sc_i}{l}\right)fm_e + \left(\frac{\theta}{H}m_e\right)' + \hat{A}_eEm_e\right]\times\left[\theta' + \left(\frac{2}{5}\right)\hat{A}_e\hat{E}H\right] = -\Gamma_1\beta m_e\left(\beta - \frac{\theta}{H}\right) \tag{36}$$

In the derivation of the preceding equations, it has been assumed that

$$(\rho\mu)/(\rho\mu)_s = l = \text{const} \tag{37}$$

Also Pr and Sc_i have been considered constant. The parameters Γ_1 and Γ_2 are defined as

$$\Gamma_1 = \frac{\alpha_2}{5(2)^{1/2}}\left(\frac{Sc_i}{l}\right)\left(\frac{L}{u_\infty}\right)\left(\frac{M_e}{M_i}\right)^{1/2}\sigma_{eg}\hat{v}_e p^{1\to 0}(1 - e^{-\theta_v/T_g})n_{gs} \tag{38}$$‡‡

$$\Gamma_2 = \frac{1}{(2)^{1/2}}\left(\frac{Sc_i}{l}\right)\left(\frac{L}{u_\infty}\right)\frac{k_{RO}}{(T_{gs})^{1.5}}n_{es} \tag{39}$$

where k_{RO} is the constant portion of the specific recombination coefficient given in Eq. (10). The parameters Γ_1 and Γ_2 defined by Eqs. (38) and (39), respectively, represent the characteristic ratios of the electron energy conduction time to the electron-neutral gas temperature equilibration time, and the ionized-species diffusion time to the electron-ion recombination time. These two parameters define the nonequilibrium features of the shock layer with respect to the electron temperature and the electron-ion recombination.

Now, let us consider the boundary conditions for the preceding equations. The boundary conditions for the over-all governing equations, Eqs. (31) and (32), are the well-known no-slip conditions at the wall and the Hugoniot shock conditions at the shock which become as follows in terms of the transformed variables[10]:

$$\left.\begin{aligned} f(0) &= f'(0) = 0 \\ H(0) &= H_w \ll 1 \end{aligned}\right\} \tag{40}$$

$$\left.\begin{aligned} f(\eta_s) &= 2^{-5/4}(\epsilon Re_s)^{1/2} \\ f'(\eta_s) &= (\tfrac{1}{2})^{1/2} \\ H(\eta_s) &= 1 \end{aligned}\right\} \tag{41}$$

There is one more boundary condition than the total order of the over-all governing equations. This extra boundary condition is needed because the nondimensional shock standoff distance η_s is not known a priori. It was shown in Ref. 11 that the boundary conditions, Eqs. (41), must be modified to account for the "shock slips" if the rarefaction becomes too large. These "shock slips" are, however, negligible for the present flow regimes wherein $Re_s \geqq 100$ and $\epsilon \sim \frac{1}{6}$.

The boundary conditions for Eqs. (33–35) are the same as those derived in Refs. 7 and 8 except that one set of the boundary conditions will be applied behind the shock (s in Fig. 1) instead of at the boundary-layer edge. Thus we have the following conditions when the surface is highly catalytic for electron-ion recombination:

$$\left.\begin{aligned} m_i(0) &= m_e(0) = 0 \\ \hat{E}(0) &= \hat{E}_w \end{aligned}\right\} \tag{42}$$§§

$$m_i(\eta_s) = m_e(\eta_s) = 1 \tag{43}$$

Let us now consider the behavior of the electron energy equation, Eq. (36), as $\eta \to 0$. The coefficient of the highest order term of Eq. (36) vanishes as $\eta \to 0$, and there the equation has a regular singularity because the electron thermal conductivity approaches zero with m_e. As was shown in the footnote for Eq. (42), the electron density at the plasma-solid interface is not, strictly speaking, zero, for the electron diffusion to the surface must take place at finite speeds.[8] The order of magnitude of m_{ew}, however, is such that we should let $m_{ew} = 0$ in order to make the macroscopic continuum description of the present analysis self-consistent. Physically, letting $m_{ew} = 0$ in Eq. (36) simply implies that, as the electron density and therefore the electron-electron collision frequency decrease, the electron energy transfer due to the thermal conduction becomes negligibly small as compared to that due to the diffusive transport of the electrons. Thus, near the wall where $m_{ew} \to 0$, the energy loss of diffusing electrons is equal to the work done by the electrons against the electric field (the electric potential difference).¶¶ If we now specify that Eq. (36) be bounded, and thus θ_w'' be finite, the equation degenerates at the wall to

$$\theta_w' = -[Le_i/(2 + Le_i)]\tfrac{2}{5}\hat{A}_e(\hat{E}H)_w \tag{44}$$

which, when both sides are multiplied by a suitable current density, expresses the previously stated physical phenomena. A unique value of θ_w'' can be deduced from Eq. (36) by the use of the boundedness requirement and the L'Hospital's rule. The boundary conditions for Eq. (36) are now specified as

$$\left.\begin{aligned} &\theta_w'' \text{ is bounded} \\ &\theta(\eta_s) = 1 \end{aligned}\right\} \tag{45}$$

It is seen that Eq. (44) becomes the boundary condition $\theta_w' = 0$ employed in Ref. 7 when $\hat{E}$ is neglected as was done in that reference.

‡‡ In view of the uncertainties in the available values for $p^{1\to 0}$, we consider $p^{1\to 0}(1 - e^{-\theta_v/T_g})$ as constant. Γ_1, therefore, is a constant parameter.

§§ It was shown in Ref. 8 that, for metallic surfaces that are believed to be highly catalytic for electron-ion recombination,

$$m_{ew} \sim \left(\frac{M_e}{M_i}\right)^{1/2}\left(\frac{j_e}{j_i}\right)_w\left(\frac{\hat{\lambda}_{egw}}{y_s}\right) \qquad m_{iw} \sim \left(\frac{\hat{\lambda}_{igw}}{y_s}\right)$$

¶¶ Note that this is basically the gross energy relationship one satisfies in the classical collisionless sheath analysis.[1, 2] The rate of diffusion of electrons at the surface, however, is governed by the electron-neutral gas collisions as well as the electric field in the present analysis, whereas it is governed by such as the free-fall conditions in the classical cases.

With all of the boundary conditions having been described, the governing equations for the shock layer, Eqs. (31–36), are solved by the use of a digital computer. As was mentioned earlier, the over-all momentum and energy equations, Eqs. (31) and (32), are decoupled from the rest of the equations. These two equations are, therefore, first integrated by the method described in Ref. 10.

The four coupled nonlinear equations, Eqs. (33–36), constitute a formidable set to be integrated, especially for the large values of $\hat{A}$. An integration scheme was devised for the IBM 7094 digital computer to solve the equations by Holt and Riley,* and the major features of the program are given in the Appendix of Ref. 24.

Region Between Shock Layer and Freestream

In order to relate the shock-layer solutions to the freestream conditions, Eqs. (23) and (24) must be solved.

With their last two terms neglected (see Sec. II), Eqs. (23) and (24) are ordinary differential equations. Equation (23) can be immediately integrated to give

$$\frac{dp_e}{dr} + en_eE^* = -v_en_e\left(\frac{kT_e}{D_e}\right) = \frac{B_0}{(r/L)^2} = \frac{B_0}{R^2} \quad (46)$$

where

$$B_0 = -\left(v_en_e\frac{kT_e}{D_e}\right)_0 = \left(\frac{ekn_eT_e}{L}\right)_s 2^{1/4}\left(\frac{Re_s}{\epsilon}\right)^{1/2}\left[\left(\frac{\theta}{H}m_e\right)' + \hat{A}_e\hat{E}\right] \quad (47)$$

In order to integrate Eq. (24) analytically, we make the following approximations. First, we replace the function $(1/n_e)(dn_e/dR)$ by a delta function $(\ln 1/\epsilon)\cdot\delta(R)$ as was done in Ref. 22. The justification of the replacement comes from the fact that the thickness of the ion shock is much smaller than the region through which the electron temperature varies. Next, we assume that the electron thermal conductivity λ_e is constant in the inviscid region at some suitable value $\hat{\lambda}_e$. The energy equation, Eq. (24), can now be integrated between $R = 1$ and ∞ with the aid of Eq. (46), and the following two equations result for the regimes $-v_e \ll u_\infty$ and $-v_e \gg u_\infty$, respectively:

$$\theta_\infty = I_1(e^{3B_2/2})\left[2^{1/4}\left(\frac{Re_s}{\epsilon}\right)^{1/2}\theta_s' + \frac{10}{3}\left(\frac{1}{Le_i}\right)B_1 - B_2\ln\frac{1}{\epsilon}\right] + 1 - \frac{10}{3}\left(\frac{1}{Le_i}\right)B_1 \quad (48)$$

$$\theta_\infty = 1 - \frac{10}{3}\left(\frac{1}{Le_i}\right)B_1 + \frac{(1 - e^{-3B_1/2})}{(3B_1/2)} \times \left[2^{1/4}\left(\frac{Re_s}{\epsilon}\right)^{1/2}\theta_s' + \frac{10}{3}\left(\frac{1}{Le_i}\right)B_1 - B_1\ln\frac{1}{\epsilon}\right] \quad (49)$$

where

$$B_1 = \frac{1}{5}2^{1/4}Le_i\left(\frac{Re_s}{\epsilon}\right)^{1/2}\left[\left(\frac{\theta}{H}m_e\right)' + \hat{A}_e\hat{E}\right]_s$$

$$B_2 = \frac{1}{5}\beta Re_sPr\left(\frac{M_e}{M_i}\right)^{1/2} + B_1 \quad (50)$$

$$I_1 = e^{-3B_2/2} + \left(\frac{3B_2}{2}\right) \times \left[0.57721 + \ln\left(\frac{3B_2}{2}\right) - \left(\frac{3B_2}{2}\right) + \frac{(3B_2/2)^3}{2\cdot 2!}\cdots\right]$$

In deriving the preceding final forms, we chose $\hat{\lambda}_e = \lambda_{e0}$.

* Mathematicians at the Aerospace Corporation.

Each of the numerical shock-layer solutions gives the values of all the parameters appearing on the right-hand sides of Eqs. (48) and (49). Therefore, each shock-layer solution can now be related to a particular freestream electron temperature except when $-v_e \approx u_\infty$. This last regime comprises only a small portion of the total surface potential spectrum, and the solutions for $-v_e \approx u_\infty$ are not essential in constructing a potential-current characteristic curve.

Electric Currents and Potential Differences

With the solutions of the governing equations available, the surface current density and the potential difference can be obtained from the following nondimensional equations:

$$J = \frac{(j_e - j_i)_w}{(l/Sc_i)2^{1/4}(Re_s/\epsilon)^{1/2}(\nu_s/L)n_{es}} = \frac{1}{\beta}\left(\frac{M_i}{M_e}\right)^{1/2}\left(\frac{\theta}{H}\right)_w m_{ew}' - m_{iw}' \quad (51)$$

$$\frac{e(V_w - V_\infty)}{kT_{gs}} = \frac{1}{\beta}\left[\underbrace{\hat{A}_e\int_0^{\eta_s}\hat{E}Hd\eta}_{\text{Shock Layer}} + \underbrace{\ln\frac{1}{\epsilon}}_{\text{Shock}} + \underbrace{\frac{5}{Le_i}B_1 + 1 - \theta_\infty}_{\text{Upstream}}\right] \quad (52)$$

Equation (52) is derived by integrating electric field intensity between w and ∞. Note the contributions of various flow regions to the potential difference.

Numerical Solutions Obtained

The numerical solutions are obtained herein in order to establish typical potential-current relationships for ionized air and to study the effects of the major parameters on the electrical characteristics.

All of the solutions obtained are for $H_w = 0.05$, $\epsilon = 0.16$, $Pr = 0.72$, $Sc_i = 0.52$, and $l = 1$. The equations are solved for Re_s of 100 and 500, and $\hat{A}_i$ of 113.5 and 1,135. Γ_1 and Γ_2 are varied between 0 and 0.2. The particular combinations of Re_s and $\hat{A}_i$ for which the solutions are obtained correspond to A_i of between 10^5 and 5×10^6. These values of A_i represent the electron number densities between about 5×10^{10} and $3 \times 10^{12}/\text{cm}^3$ at s† when T_{es} and T_{gs} are in the order of $10^4 K$.

The numerical solutions obtained are examined to see if they satisfy the three continuum plasma criteria set forth at the beginning of Sec. II. It was found that the criteria are well satisfied for all the cases considered herein for typical laboratory conditions‡ except for the lowest values of n_{es} when the surface potential is such that the electron current is excessive. It was found that the ratio of the characteristic electron-electron collision time to the characteristic electron residence time approaches order one, thus violating the last criterion, as J approaches 100 when n_{es} is 5×10^{10} and $L \sim \frac{1}{2}$ in.

IV. Discussion

Let us first investigate the magnitude of the parameters Γ_1 and Γ_2, which one would encounter in a laboratory diagnostic work. When the ionized stream is air, and when $L \sim \frac{1}{2}$ in., and $n_{gs} \sim 10^{17}/\text{cm}^3$, Γ_1 and Γ_2 are found to be smaller than 10^{-2} and hence are negligible for all the cases solved herein. In computing Γ_1, the probability factor $p^{1\to 0}(1 - e^{-\theta_v/T_g})$ for energy transfer between electrons and the vibrational states of O_2 and N_2 was considered to be 100 times that for the elastic collisions, and α_2 was set equal to

† Note that $n_{e\infty} = \epsilon n_{es}$.

‡ See Ref. 24 for details.

1. It can be seen in Massey and Burhop[17] that, for the electron energies up to about 2 ev, the maximum probability of the energy transfer by the inelastic encounter is about 100 times of that due to the elastic collisions. Also, α_2 will be very small as compared to 1 in most of the high-temperature experimental facilities. Therefore, the values of Γ_1 computed herein represent the upper limits, and, for most of the probe operations in pure air, the temperature equilibration process between the electrons and the neutral gases may be considered frozen.

As it is seen from Eq. (39), Γ_2 is proportional to n_{es}. The magnitude of Γ_2, therefore, will increase and become nonnegligible as n_{es} increases beyond those considered herein.

Before we discuss the numerical results, let us consider the basic behavior of the potential-current relationship that we may expect. For $\Gamma_2 = 0$, we derive the following equations for J and $(j_e/j_i)_w$ in terms of the conditions at the sheath edge (Δ) by assuming that the convection is negligible within the sheath:

$$J = \frac{1}{(M_e/M_i)^{1/2}} \times \left\{ \frac{1 + (M_e/M_i)^{1/2}}{1 + (M_e/M_i)^{1/2}(j_e/j_i)_w} \left[\left(\frac{M_e}{M_i}\right)^{1/2} \left(\frac{j_e}{j_i}\right)_w m_\Delta' - \left(\frac{T_e}{T_g}\right)_s \times \left(\frac{\theta}{H} m\right)_\Delta' \right] - \left[\left(\frac{M_e}{M_i}\right)^{1/2} m_\Delta' - \left(\frac{T_e}{T_g}\right)_s \left(\frac{\theta}{H} m\right)_\Delta' \right] \right\} \quad (53)$$

$$\left(\frac{j_e}{j_i}\right)_w = \left(\frac{M_i}{M_e}\right)^{1/2} \left\{ \frac{l \mu_s}{Sc_i} \frac{2^{1/4}}{L} \left(\frac{Re_s}{\epsilon}\right)^{1/2} \frac{n_{es}}{\rho_s} \frac{1}{j_{iw}} \times \left[m' + \left(\frac{T_e}{T_g}\right)_s \left(\frac{\theta}{H} m\right)' \right]_\Delta - 1 \right\} \quad (54)$$

For highly negative and highly positive surface potentials we obtain from Eq. (53), when $(j_e/j_i)_w \ll 1$,

$$J = -\left[\left(\frac{T_e}{T_g}\right)_s \left(\frac{\theta}{H} m\right)' + m' \right]_\Delta \quad (55)\S$$

and when $(M_e/M_i)^{1/2} (j_e/j_i)_w \gg 1$,

$$J = \left(\frac{M_e}{M_i}\right)^{1/2} \left[\left(\frac{T_e}{T_g}\right)_s \left(\frac{\theta}{H} m\right)' + m' \right]_\Delta \quad (56)$$

The following observations can be made from the preceding relationships independently of the probe shapes and sizes by noticing the fact that m_Δ' is quite insensitive to $(j_e/j_i)_w$. For highly negative surface potentials, (T_e/T_g) will reach a limit because the value of electron energy sink term E^*, j_e approaches a limit as $j_e \to 0$. Therefore, according to Eq. (55), the ion saturation current will always be obtained. For highly positive surface potentials, on the other hand, an electron saturation current will be obtained only if the electron-neutral gas temperature equilibration process is such that (T_e/T_g) is constant throughout the flow field and is also invariant with respect to surface potential. When $\Gamma_1 \to 0$, the positive electric field penetrating into the inviscid region must heat the electrons as it creates the electron diffusion current toward the shock [see Eq. (19)]. Hence, $(T_e/T_g)_s$ increases with J, which in turn, according to Eq. (56), increases with the surface electrical bias when $(T_e/T_g)_s$ is variable. Therefore, an electron saturation current in the classical sense is not usually obtained when $\Gamma_1 \to 0$. This point is seen to be in contrast with the classical sheath theories.[1, 2] However, the preceding argument is consistent with the continuum theories such as Ref. 5 wherein an electron saturation current was predicted when T_e/T_g was assumed to be constant. Recently Starner,[23] in his experimental work with argon, found that the electron current increased continuously with the potential up to values much greater than those predicted by the existing theories.

§ Note, $m_{i\Delta}' = m_{e\Delta}' = m_\Delta'$

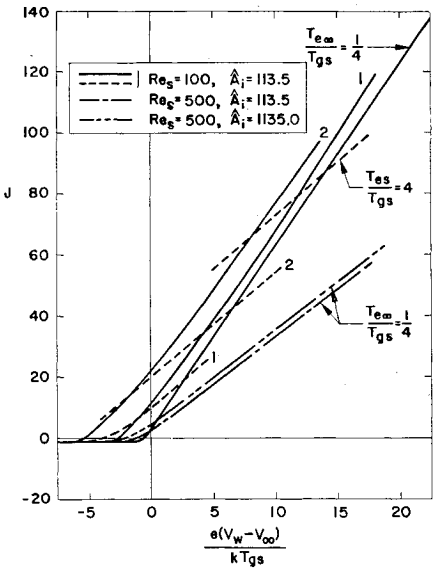

Fig. 2 Current-potential relationships for $\Gamma_1 = \Gamma_2 = 0$.

In practice, Γ_1 is not strictly zero and, for sufficiently large values of $(T_e - T_g)$, the electron energy loss to the neutrals by collisions will limit T_e and hence will eventually limit the electron current. Also, at sufficiently high electron temperatures, the ionization of neutrals by electrons will change the situation from that considered herein.

It should be remembered that the preceding arguments concerning the saturation currents are based on the assumption that the probe is located in an infinite, flowing plasma, which can supply all the electrons required by J without disturbing the freestream (∞). When the plasma jet is relatively small or the other electrode is located near the probe, the present argument fails because the freestream plasma may become biased and limit the electron supply.

Figure 2 shows the typical potential-current characteristic curves for $\Gamma_1 = \Gamma_2 = 0$. It is first seen that the nondimensional ion saturation current $(-J)_{sat}$ is insensitive to the parameters $T_{e\infty}$, Re_s, $\hat{A}_i$, etc. Hence, from Eq. (51), $(j_{iw})_{sat} \sim n_{es}(Re_s)^{1/2}$. In fact, $(-J)_{sat}$ varied between 0.95 and 1.15 for the cases computed herein. Therefore, one should be able to deduce $n_{e\infty}$ readily from the measured values of ion saturation current by the use of Eq. (51).

Although $(-J)_{sat}$ is rather insensitive to the parameters such as $T_{e\infty}$ and Re_s, the other values of J vary with these parameters. Once $n_{e\infty}$ is determined from the ion saturation current, therefore, the measurement of either the floating potential or J for $V_w = V_\infty$ may be used to determine $T_{e\infty}$.

Figure 2 shows that, for a given $T_{e\infty}$, the electron temperature near the shock continuously increases as does the surface potential. Figure 3 shows two sets of typical m_i, m_e, E, H, and (T_e/T_{gs}) profiles for the shock layer corresponding to the $(T_{e\infty}/T_{gs}) = 2$ line of Fig. 2. In this particular case, the electron temperature behind the shock is doubled as $e(V_w - V_\infty)/kT_{gs}$ is raised from -3.26 to 7.43. As we see, the numerical results compliment the previous arguments on the continuously increasing electron current based on the increasing T_{es}.

Figure 4 shows the effects of the finite rate electron-neutral gas temperature equilibration and the electron-ion recombination on the potential-current relationship. As $(T_e - T_g)$ increases with the surface potential for $\Gamma_1 = 0.2$ and $\Gamma_2 = 0$, the collisional energy loss of electrons to the neutrals begins to limit the electron current as was mentioned earlier. For $\Gamma_1 = 0$, $\Gamma_2 = 0.2$, both the electron and ion currents to the surface are reduced because of the depletion of the charged

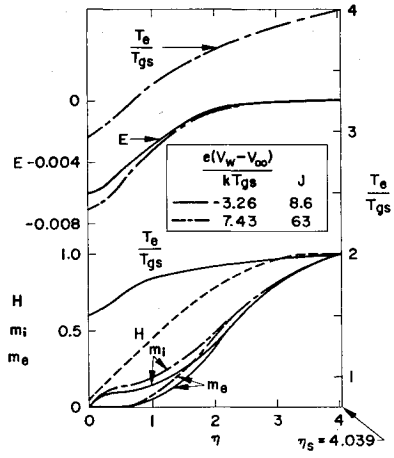

Fig. 3 Typical shock-layer profiles for $Re_s = 100$, $\hat{A}_i = 113.5$, $\Gamma_1 = \Gamma_2 = 0$, and $T_{e\infty}/T_{gs} = 2$.

particles by the chemical reaction. With the increasing surface potential, the electron-ion recombination process is seen to freeze, and hence the solid and the broken lines are seen to merge together. The main reason for this is that, for a given value of Γ_2, the over-all recombination rate varies with $T_e^{-1.5}$ because $k_R \sim T_e^{-1.5}$.

Figures 5 and 6 show the effects on the profiles of the collisional energy exchange between electrons and neutrals and of the nonequilibrium electron-ion recombination, respectively. These effects are shown for the given surface electric field intensities. It is seen from the figures that Γ_1, which affects the electron temperature greatly, has very little effect on m_i and m_e; and Γ_2, which affects m_i and m_e substantially, has only a moderate effect on T_e.

The broken lines in Fig. 6 are included to show the effect of surface potential on the general shape of the electron temperature profile in the shock layer. A comparison of the solid and the broken lines shows that the electron temperature variation due to the electric field is rather confined to the region adjacent to the wall when electric current is small,¶ but the variation spreads throughout the shock layer as the surface potential and the electron current are increased. The main reason for this is that, when the surface is highly negative such that j_e is small, the electron concentration and therefore λ_e are also very small near the wall. Thus, the electron temperature depression created by the strong electric field in the sheath cannot affect the electron temperatures in the rest of the shock layer greatly. With the increasing

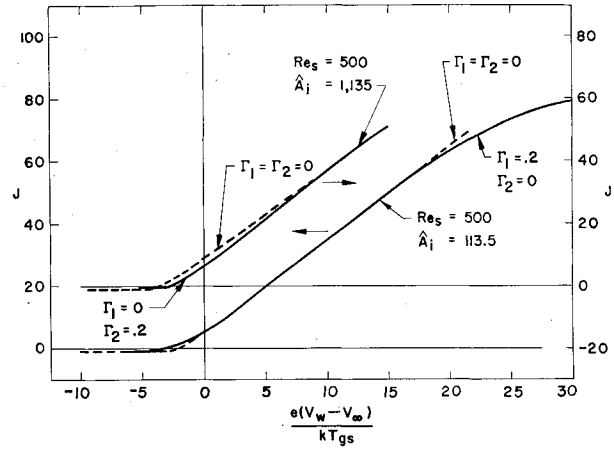

Fig. 4 Current-potential relationships for $T_{e\infty}/T_{gs} = \frac{1}{4}$ showing the effects of Γ_1 and Γ_2.

¶ This shows that the assumption made in Ref. 7 of neglecting the E^* term in the energy equation of the viscous layer, when ϵ is small, is fairly well justified.

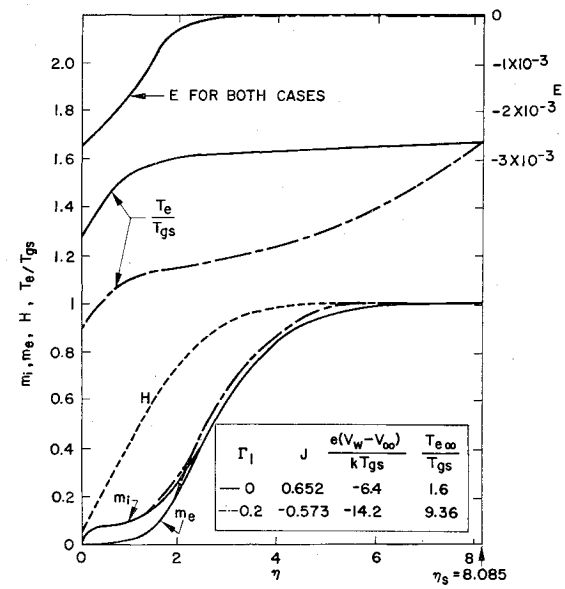

Fig. 5 Typical shock-layer profiles for $Re_s = 500$, $\hat{A}_i = 113.5$, $E_w = -0.00268$, and $\Gamma_2 = 0$.

j_e, λ_e is increased in the sheath, and the electron temperature disturbance near the wall is quickly spread throughout the shock layer.

V. Concluding Remarks

The electrochemical interactions between the hypersonic stream of weakly ionized gases and the stagnation region of an electrically biased axisymmetric blunt body have been analyzed. The analysis was based on a continuum description. From the study, typical current-potential relationships for electrostatic stagnation probes have been obtained. Also, the effects of the major governing parameters on the electrical interactions have been determined.

When both the collisional energy exchange between electrons and neutrals and the electron-ion recombination are frozen, the nondimensional saturated ion current is insensitive to the governing parameters. Also, for the surface potential above the floating value, the electron temperatures near the shock continuously increase with the surface potential and, because of this, no definite electron saturation current predicted by the previous theories is usually reached. In practice, however, the electron current may become limited due to such effect as the electron energy loss to the neutrals by collisions. These points have been elaborated in the preceding section.

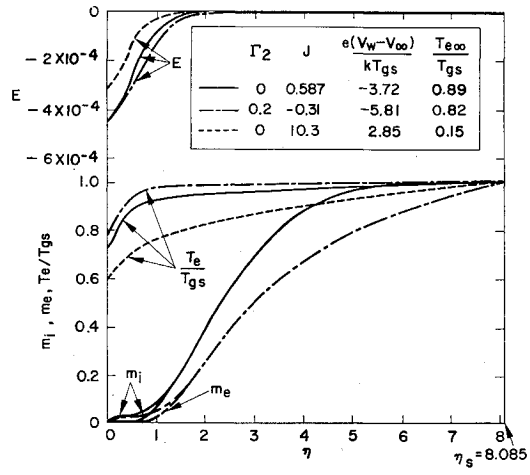

Fig. 6 Typical shock-layer profiles for $Re_s = 500$, $\hat{A}_i = 1{,}135$, $E_w = -0.000447$, and $\Gamma_1 = 0$.

Finally, the potential of an inviscid plasma varies with the electron temperature. Therefore, in a laboratory practice, if the other electrode (supposedly at ∞) is situated such that it is in an electrical contact with the stagnation chamber of an arc facility or the plasma near the shock where the electron temperature is much higher than that at the test section, one would find the measured characteristic curves located toward the left of the present curves such as Fig. 2. This is due to the increased reference potential. Under such circumstances, of course, one will not be measuring anything at the test section.

In closing, the guard electrode (see Fig. 1) was considered to be electrically floating in the work of Ref. 24. The resulting potential-current characteristics for $J > 0$ were therefore numerically different from those of the present study. The general basic features found in Ref. 24, however, were the same as the present ones.

References

[1] Cobine, J. D., *Gaseous Conductors* (Dover Publications, Inc., New York, 1958), Chap. VI.

[2] Talbot, L., "Theory of stagnation-point Langmuir probe," Phys. Fluids **3**, 289–298 (1960).

[3] Turcotte, D. L., "The effect of electric and magnetic fields on electron heat transfer," AIAA Preprint 63-461 (1963).

[4] Wilson, D. S. and Turcotte, D. L., "Electrical resistance and sheath potential of a cold electrode in a shock tube with an applied magnetic field," *Proceedings of the 5th Symposium on Engineering Aspects of MHD* (MIT Press, Cambridge, Mass., 1964), pp. 149–160.

[5] Lam, S. H., "General theory for the flow of weakly ionized gases," AIAA Preprint 63-459 (1963).

[6] Su, C. H., "Compressible plasma flow over a biased body," Massachusetts Institute of Technology Fluid Mechanics Lab. Publ. 64-3 (1964).

[7] Chung, P. M. and Mullen, J. F., "Nonequilibrium electron temperature effects in weakly ionized stagnation boundary layers," Aerospace Corp. Rept. TDR-169(3230-12) TN-7 (1963); also AIAA Paper 63-161 (1963).

[8] Chung, P. M., "Electrical characteristics of Couette and stagnation boundary layer flows of weakly ionized gases," Phys. Fluids **7**, 110–120 (1964).

[9] Hayes, W. D. and Probstein, R. F., *Hypersonic Flow Theory* (Academic Press Inc., New York, 1959), Chap. X.

[10] Chung, P. M., "Hypersonic viscous shock layer of nonequilibrium dissociating gas," NASA TR R-109 (1961).

[11] Cheng, H. K., "The blunt-body problem in hypersonic flow at low Reynolds numbers," IAS Paper 63-92 (1962).

[12] Wasserstrom, E., Su, C. H., and Probstein, R. F., "A kinetic theory approach to electrostatic probes," Massachusetts Institute of Technology Fluid Mechanics Lab. Publ. 64-5 (May 1964).

[13] Chung, P. M., "Chemically reacting nonequilibrium boundary layers," *Advances in Heat Transfer* (Academic Press Inc., New York, 1964), Vol. II.

[14] Camac, M. and Kemp, N. H., "A multitemperature boundary layer," AIAA Preprint 63-460 (1963).

[15] Dix, D. M., "Energy transfer processes in a partially ionized, two-temperature gas," Aerospace Corp. Rept. ATN-64 (9232)-1 (1964).

[16] Lin, S. C. and Teare, J. D., "Rate of ionization behind shock AVCO-Everett Research Rept. 115 (1962).

[17] Massey, H. S. W. and Burhop, E. H. S., *Electronic and Ionic Impact Phenomena* (Clarendon Press, Oxford, England, 1952), Chap. IV.

[18] Schulz, G. J., "Vibrational excitation of nitrogen by electron impact," Phys. Rev. **125**, 229–232 (1962).

[19] Herzfeld, K. F. and Litovitz, T. A., *Absorption and Dispersion of Ultrasonic Waves* (Academic Press Inc., New York, 1959), Chap. II.

[20] Fay, J. A., "Plasma boundary layers," ARS Preprint 2010-61 (1961).

[21] Hansen, C. F., "Approximations for the thermodynamic and transport properties of high-temperature air," NASA TR R-50 (1959).

[22] Grewal, M. D. and Talbot, L., "Shock-wave structure in a partially ionized gas," J. Fluid Mech. **16**, 573–594 (1963).

[23] Starner, K., private communication, Aerospace Corp., El Segundo, Calif. (May 1964).

[24] Chung, P. M., "Weakly ionized nonequilibrium viscous shock layer and electrostatic probe characteristics," Aerospace Corp. Rept. TDR-269(S4230-40)-1 (July 1964).